

**TECHNICAL EVALUATION OF THE SIEMENS NOVATION
FULL FIELD DIGITAL MAMMOGRAPHY SYSTEM**

**NHSBSP Equipment Report 0710
December 2007**

**K C Young and J M Oduko
National Coordinating Centre for the Physics of Mammography**

Enquiries

Enquiries about this report should be addressed to:

Professor KC Young

National Coordinating Centre for the Physics of Mammography

Medical Physics Department

Royal Surrey County Hospital

Guildford

GU2 7XX

Tel: 01483 406738

Fax: 01483 406742

Email: ken.young@nhs.net

Published by

NHS Cancer Screening Programmes

Fulwood House

Old Fulwood Road

Sheffield

S10 3TH

Tel: 0114 271 1060

Fax: 0114 271 1089

Email: nhs.screening@cancerscreening.nhs.uk

Website: www.cancerscreening.nhs.uk

© NHS Cancer Screening Programmes 2007

The contents of this document may be copied for use by staff working in the public sector but may not be copied for any other purpose without prior permission from the NHS Cancer Screening Programmes.

The report is available in PDF format on the NHS Cancer Screening Programmes' website

Typeset by Prepress Projects Ltd, Perth (www.prepress-projects.co.uk)

Printed by Charlesworth

CONTENTS

| | Page No |
|--|----------------|
| ACKNOWLEDGEMENTS | v |
| 1. INTRODUCTION | 1 |
| 1.1 Testing procedures and performance standards for digital mammography | 1 |
| 1.2 Objectives | 1 |
| 2. METHODS | 1 |
| 2.1 System tested | 1 |
| 2.2 Detector response and noise analysis | 1 |
| 2.3 Dose measurement | 2 |
| 2.4 Contrast to noise ratio | 2 |
| 2.5 Image quality measurements | 3 |
| 2.6 Optimisation | 4 |
| 3. RESULTS | 5 |
| 3.1 Detector response | 5 |
| 3.2 Noise measurements | 6 |
| 3.3 AEC performance | 8 |
| 3.4 Image quality measurements | 11 |
| 4. DISCUSSION | 19 |
| 5. CONCLUSIONS | 20 |
| REFERENCES | 20 |

ACKNOWLEDGEMENTS

The authors are grateful to the staff at the Cambridge Breast Screening Unit for their help in evaluating the unit at their centre.

1. INTRODUCTION

1.1 Testing procedures and performance standards for digital mammography

This report is one of a series evaluating commercially available digital mammography systems on behalf of the NHS Breast Screening Programme (NHSBSP). The testing methods and standards applied are mainly derived from NHSBSP Equipment Report 0604.¹ This is referred to in this document as the NHSBSP protocol and it has the same image quality and dose standards as those provided in the European protocol.^{2,3} The European protocol was followed where there is a more detailed performance standard, eg for the automatic exposure control (AEC) system.

1.2 Objectives

The purpose of these tests was to determine whether the Siemens Novation meets the main standards in the NHSBSP and European protocols, and to provide performance data for comparing this system against other manufacturers' products. Additional measurements were also undertaken to assess how well the system's AEC was optimised. The method of assessing optimisation has been reported previously.^{4,5} Clinical evaluations are published separately by the NHSBSP where systems meet the minimum standards in the NHSBSP protocol. A final decision on the suitability of systems for use in the NHSBSP depends on a review of both the technical and clinical evaluations.

2. METHODS

2.1 System tested

Some measurements were made on a Siemens Novation at the Siemens factory in Erlangen, Germany. Another unit was installed at the Cambridge Breast Screening Unit at Addenbrookes Hospital, Cambridge, for clinical evaluation. Most of the measurements were repeated on this system.

2.2 Detector response and noise analysis

The detector response was measured broadly as described in the NHSBSP protocol. A phantom of polymethyl-methacrylate (PMMA) with a total thickness of 45 mm was positioned at the tube exit port and exposed using the three target-filter combinations available at tube voltages typical of those used clinically (28 kV Mo/Mo, 28 kV Mo/Rh, 27 kV W/Rh). An ion chamber was positioned at the surface of the breast support table, and the entrance surface air kerma was measured for a range of tube current-time products for each target-filter combination tested. The readings were corrected to the surface of the imaging detector using the inverse square law. It was determined that the imaging detector is at a distance of 65 cm from the tube focus and 1.6 ± 0.1 cm below the surface of the breast support table. No correction was made for attenuation by the protective plates above the detector. However, a grid transmission factor of 0.67 was assumed and used in the calculation. The images were saved as unprocessed files and transferred to another computer for analysis. A 10 mm² region of interest (ROI) was positioned on the midline and 6 cm from the chest wall edge of each image. The average pixel value and the standard deviation of pixel values within that region were measured. The relationship between average pixel values and the detector entrance surface air kerma was determined. The magnitude of the pixel offset at zero air kerma was determined. The standard deviations of the pixel values in the ROI for each image were used to investigate the relationship between dose to the detector and image noise.

2.3 Dose measurement

Doses were measured by using the AEC to expose different thicknesses of PMMA to simulate breasts. U-shaped expanded polystyrene spacers were added to adjust the total thickness to be equal to the equivalent breast thickness. Mean glandular doses (MGDs) were calculated for the equivalent breast thicknesses and the displayed doses recorded. To measure the contrast to noise ratio (CNR), an aluminium square measuring $10 \times 10 \times 0.2$ mm was placed on top of the 20 mm thick block, with one edge on the midline and 6 cm from the chest wall edge. Additional layers of PMMA were added on top to vary the total thickness.

2.4 Contrast to noise ratio

The images of the blocks of PMMA obtained during the dose measurement were analysed to obtain the CNRs. Multiple small ROIs ($< 3 \times 3$ mm) were used to determine the average signal and the standard deviations in the signal within the image of the aluminium square and the surrounding background. Small ROIs are used to minimise distortions due to the heel effect. However, this is less important for this system because flat field correction is applied. The CNR was calculated for each image as defined in the NHSBSP and European protocols.

To apply the standards in the European protocol, the limiting value for CNR (using 50 mm PMMA) was determined according to equation 1. This equation determines the CNR value ($CNR_{\text{limiting value}}$) that is necessary to achieve the minimum threshold gold thickness for the 0.1 mm detail (ie $\text{threshold gold}_{\text{limiting value}} = 1.68 \mu\text{m}$, which is equivalent to $\text{threshold contrast}_{\text{limiting value}} = 23.0\%$ using 28 kV Mo/Mo). Threshold contrasts were calculated as described in the European protocol and used in equation 1.

$$\text{Threshold contrast}_{\text{measured}} \times CNR_{\text{measured}} = \text{Threshold contrast}_{\text{limiting value}} \times CNR_{\text{limiting value}} \quad (1)$$

The relative CNR was then calculated according to equation 2 and compared with the limiting values provided for relative CNR shown in Table 1. The minimum CNR required to meet this criterion was then calculated.

$$\text{Relative CNR} = CNR_{\text{measured}} / CNR_{\text{limiting value}} \quad (2)$$

Table 1 Limiting values for relative CNR

| Thickness of PMMA (mm) | Equivalent breast thickness (mm) | Limiting values for relative CNR (%) in European protocol |
|------------------------|----------------------------------|---|
| 20 | 21 | > 115 |
| 30 | 32 | > 110 |
| 40 | 45 | > 105 |
| 45 | 53 | > 103 |
| 50 | 60 | > 100 |
| 60 | 75 | > 95 |
| 70 | 90 | > 90 |

2.5 Image quality measurements

Contrast detail measurements were made using the CDMAM phantom (version 3.4, UMC St. Radboud, Nijmegen University, Netherlands). The phantom was positioned with a 20 mm thickness of PMMA above and below, to give a total attenuation approximately equivalent to 50 mm of PMMA or 60 mm thickness of typical breast tissue. This arrangement was imaged using the x-ray set's automatically selected factors normally set for clinical use for a breast of equivalent attenuation, ie 60 mm. This procedure was repeated seven times to obtain a representative sample of eight images. Unprocessed images were transferred to disk for subsequent analysis off site. These image quality measurements were then repeated at other dose levels by manually selecting higher and lower mAs values with the same beam quality as selected under AEC control.

For an image quality measurement at each dose level, three observers reviewed four of the digital images on a medical grade DICOM calibrated soft copy display. The contrast and brightness of each image were adjusted by the observer to optimally display the details in the test object, before scoring. The test object manufacturer's correction scheme (nearest neighbour correction) was then applied before determining the threshold gold thickness for each detail diameter.

The average threshold gold thickness for each detail diameter for each dose level (an average for four images and three observers) was fitted with a curve as described in the NHSBSP protocol. The measured threshold gold thicknesses typically have 95% confidence limits of about 10%. The threshold contrasts quoted in the tables of results are derived from the fitted curves, as this has been found to improve the accuracy.⁶

The expected relationship between threshold contrast and dose was plotted with the experimental data for the 0.1 and 0.25 mm details and is given by equation 3.

$$\text{Threshold contrast} = \lambda D^{-n} \quad (3)$$

The appropriate value of n was determined from the analysis of the noise as a function of the pixel value. In practice, this was done by finding the value of n that provided the best fit to the experimental data. D represents the MGD for a 60 mm thick standard breast equivalent to the test phantom configuration used for the image quality measurement. λ is a constant to be fitted.

An automatic method of reading the CDMAM images was also used.^{6,7} The threshold gold thickness for a typical human observer was predicted using equation 4.

$$\text{TC}_{\text{predicted}} = r \text{TC}_{\text{auto}} \quad (4)$$

where $\text{TC}_{\text{predicted}}$ is the predicted threshold contrast for a typical observer and TC_{auto} is the threshold contrast measured using an automated procedure with CDMAM images. Contrasts were calculated from gold thickness for a nominal tube voltage of 28 kV and a Mo/Mo target-filter combination as described in the European protocol. r is the average ratio between human and automatic threshold contrast determined experimentally with the values shown in Table 2.⁶

The main advantage of automatic reading is that it has the potential of eliminating observer error, which is a significant problem when using human observers. However it should be noted that at the present time the official protocols are based on human reading.

Table 2 Values of r used to predict threshold contrast

| Diameter of gold disc (mm) | Average ratio of human to automatically measured threshold contrast (r) |
|----------------------------|---|
| 0.08 | 1.40 |
| 0.10 | 1.50 |
| 0.13 | 1.60 |
| 0.16 | 1.68 |
| 0.20 | 1.75 |
| 0.25 | 1.82 |
| 0.31 | 1.88 |
| 0.40 | 1.94 |
| 0.50 | 1.98 |
| 0.63 | 2.01 |
| 0.80 | 2.06 |
| 1.00 | 2.11 |

2.6 Optimisation

A method for determining optimal beam qualities and exposure factors for digital mammography systems has been described previously and was used to evaluate this system.^{4,5} CNRs and MGDs were measured as described above using blocks of PMMA from 20 to 70 mm thick. For each thickness four tube voltage settings were used (25, 28, 31 and 34 kV) with each of the target-filter combinations available (Mo/Mo, Mo/Rh and W/Rh) and the mAs recorded. The MGDs to typical breasts with attenuation equivalent to each thickness of the PMMA were calculated as described in the NHSBSP protocol. Each exposure was designed to achieve a standard pixel value by using the AEC in automatic mAs mode. Additional CNR measurements were made with a 45 mm thickness of PMMA using the AEC selected beam quality and a wide range of manually selected mAs values. The relationship between noise and pixel values in digital mammography systems has been previously⁵ shown to be approximated by:

$$\text{Relative noise} = \frac{\sqrt{\frac{sd(bgd)^2 + sd(Al)^2}{2}}}{p} = k_i p^{-n} \quad (5)$$

where k_i is a constant and p is the average background pixel value linearised with absorbed dose to the detector. $sd(bgd)$ is the average standard deviation of pixel values in the ROIs over the background. $sd(Al)$ is the average standard deviation of pixel values in an ROI over a $0.2 \times 10 \times 10$ mm piece of aluminium. The value of n was found by fitting this equation to the experimental data. Equation 6 was then used to calculate the dose required to achieve a target CNR, where k is a constant to be fitted and D is the MGD for a breast of equivalent thickness.

$$\text{CNR} = kD^n \quad (6)$$

The target CNR was that calculated to reach either the minimum or achievable image quality in the NHSBSP and European protocols using the following relationship

$$\text{Threshold contrast} = \frac{\lambda}{\text{CNR}} \quad (7)$$

where λ is a constant that is independent of dose, beam quality and the thickness of attenuating material. The optimal beam quality for each thickness was selected as that necessary to achieve the target CNR for the minimum dose.

3. RESULTS

3.1 Detector response

The detector was found to have a linear response with a pixel value offset of 63 as shown in Figure 1. The gradient was measured to be 0.195 μGy per pixel value at 27 kV W/Rh. The exposures selected by the AEC resulted in average pixel values of about 360 for the system in Erlangen and about 275 for the system in Cambridge. A standard value of 360 was chosen to determine the reference entrance air kerma, which was 57.8 μGy using 27 kV W/Rh in Erlangen. In practice, attenuation by protective plates will make the true value somewhat lower than this. The corresponding reference entrance air kerma values to produce pixel values of 360 using other beam qualities are shown in Figure 2.

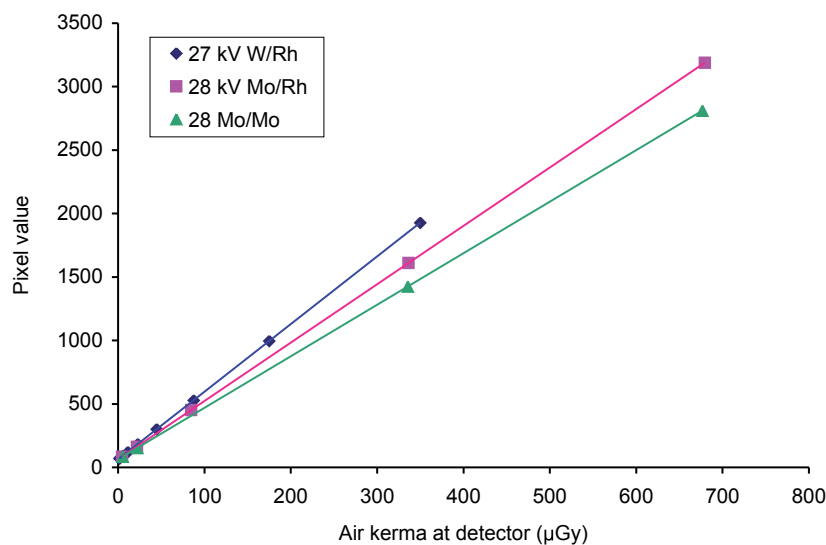


Figure 1 Detector response (Erlangen system).

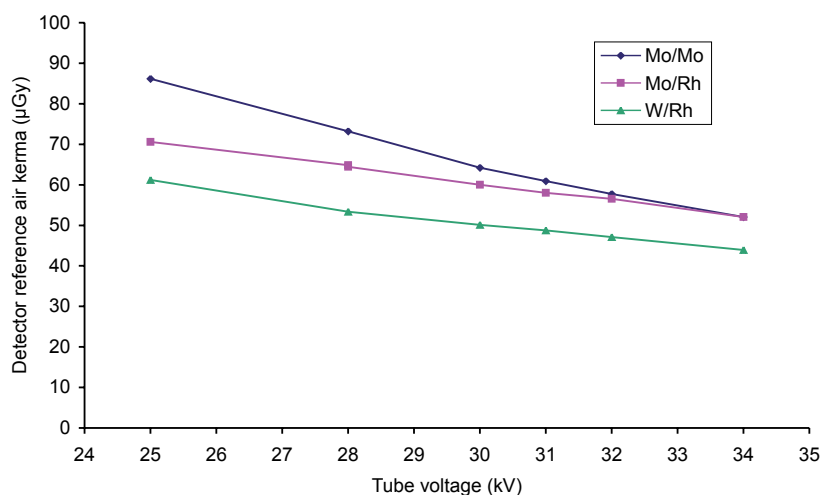


Figure 2 Detector reference air kerma for a pixel value of 360 (Erlangen system).

3.2 Noise measurements

The variation in noise with dose was analysed by plotting the standard deviation in pixel values against the detector entrance air kerma as shown in Figure 3. The fitted power curve has an index of 0.412. If only quantum noise sources were present, the data would form a straight line with an index of 0.5. The presence of some electronic noise and structural noise has caused the curve to deviate from a straight line. This is normal for such systems and quantum noise was the dominant noise source.

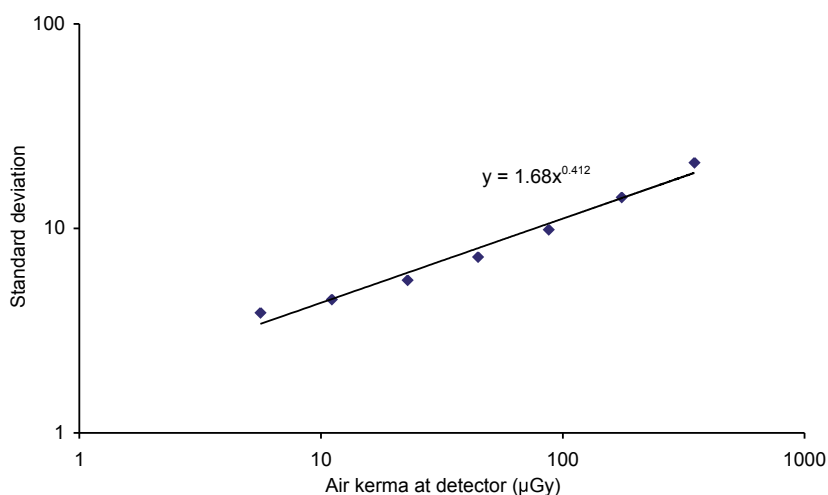


Figure 3 Standard deviation of pixel values versus air kerma at detector (Erlangen system).

The relative noise is plotted against the background pixel value (after removing the offset) in Figure 4. The offset corrected pixel value is proportional to the dose absorbed by the detector. A curve of the form described in equation 5 with an index $n = 0.498$ has been fitted to the measured data (a value of $n = 0.5$ would be expected if only quantum noise were present).

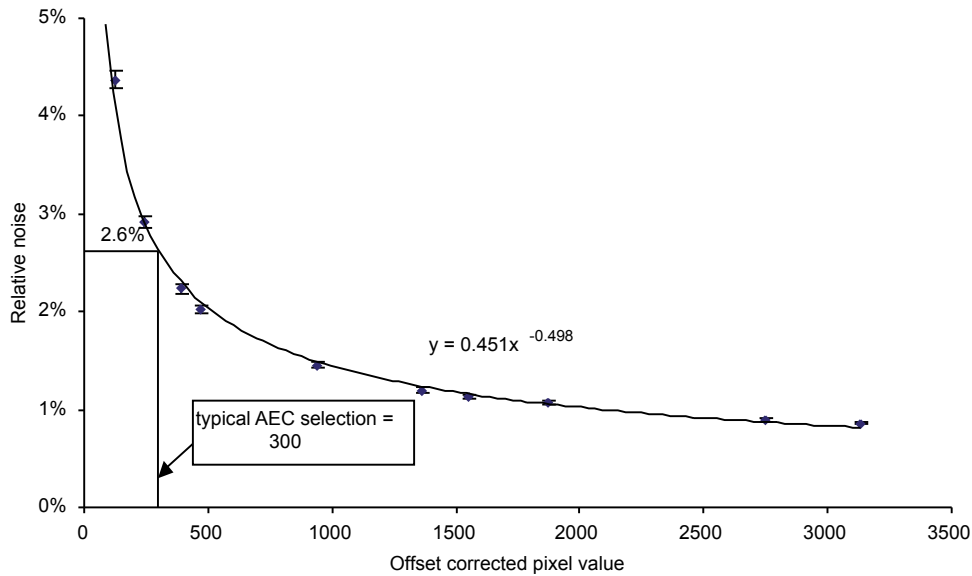


Figure 4 Relative noise at different pixel values (Erlangen system).

Figure 5 is an alternative way of presenting the data and shows the relative noise at different average pixel values. The estimated relative contributions of electronic, structural and quantum noise are shown and the quadratic sum of these contributions fitted to the measured noise.

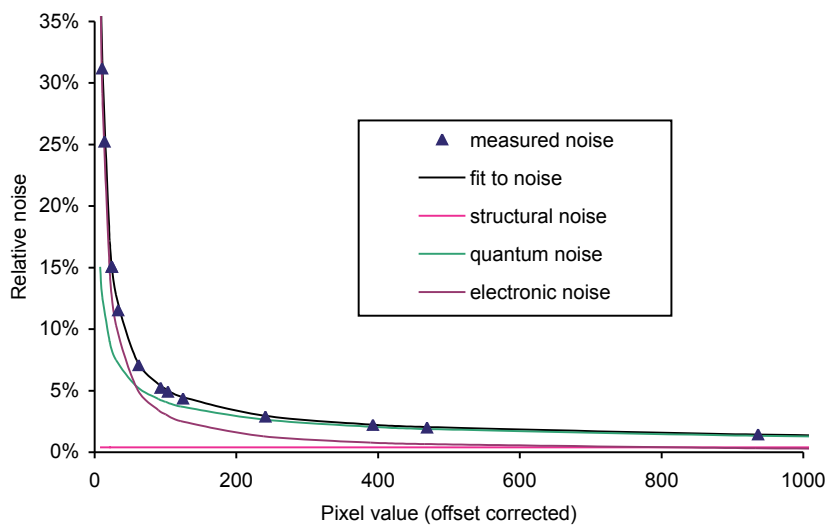


Figure 5 Relative noise and noise components at different pixel values (Erlangen system).

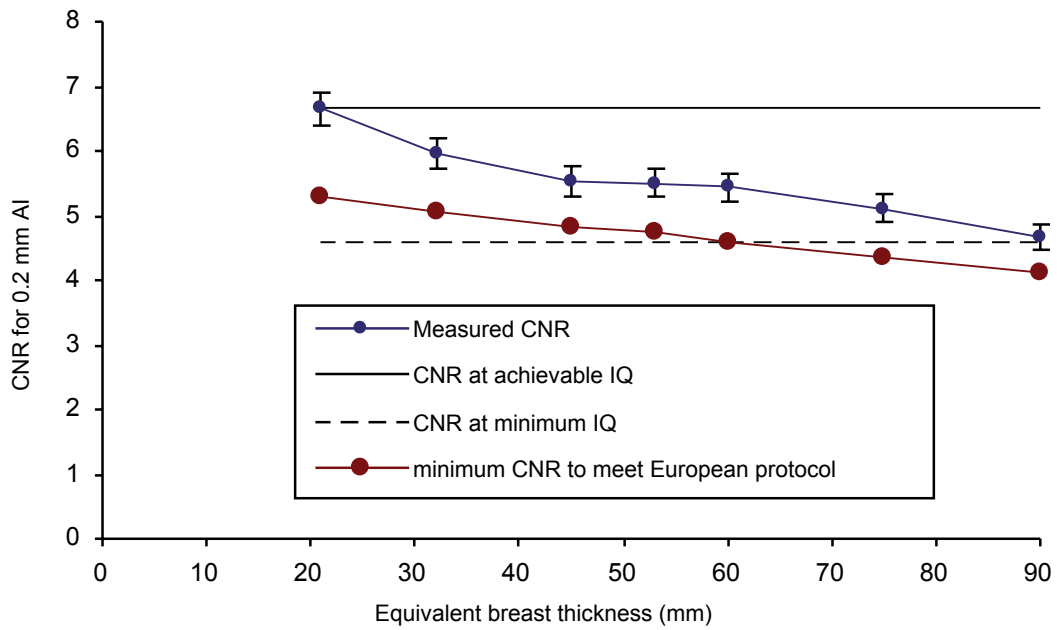


Figure 7a Measured CNR compared with limiting values in the European protocol for the system at Erlangen. Error bars indicate 95% confidence limits.

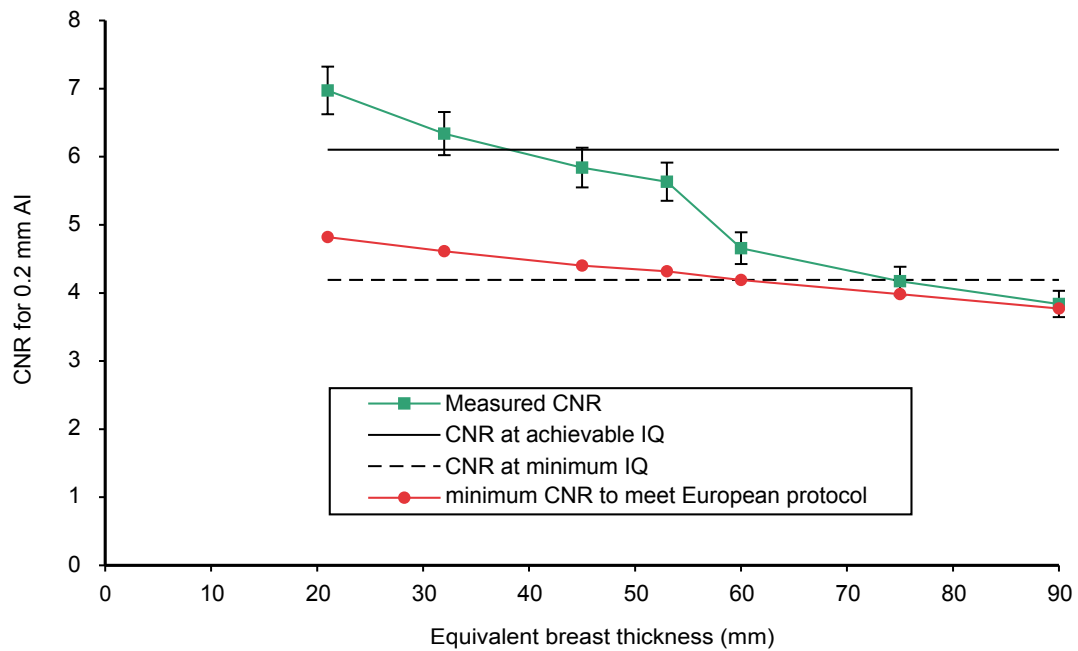


Figure 7b Measured CNR compared with the limiting values in the European protocol for the system at Cambridge. Error bars indicate 95% confidence limits.

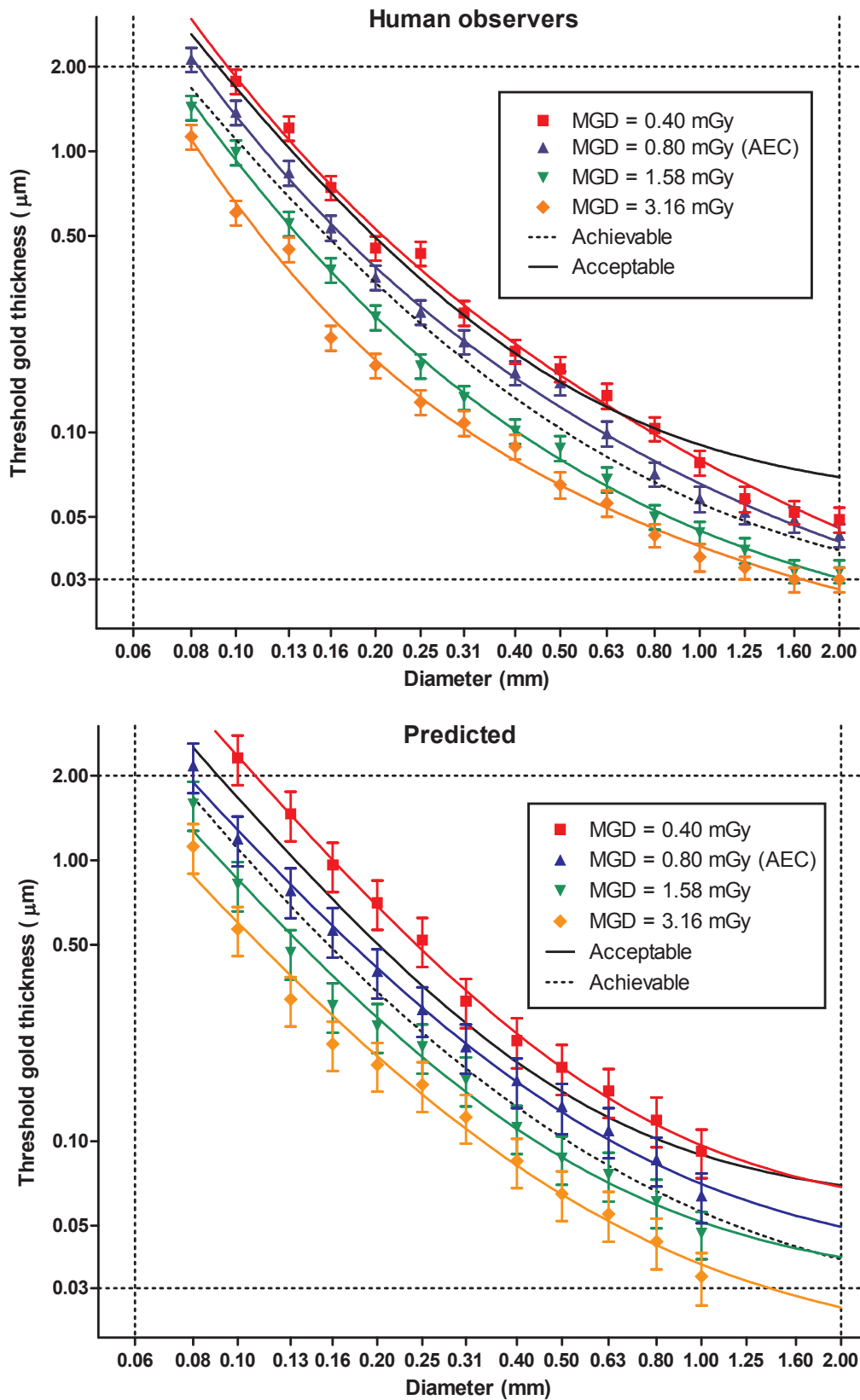


Figure 8 Contrast–detail curves for the system at Erlangen for four different doses at 28 kV W/Rh using human readers and predicted results using automated reading. The 0.80 mGy dose corresponds to the AEC selection. Error bars indicate 95% confidence limits.

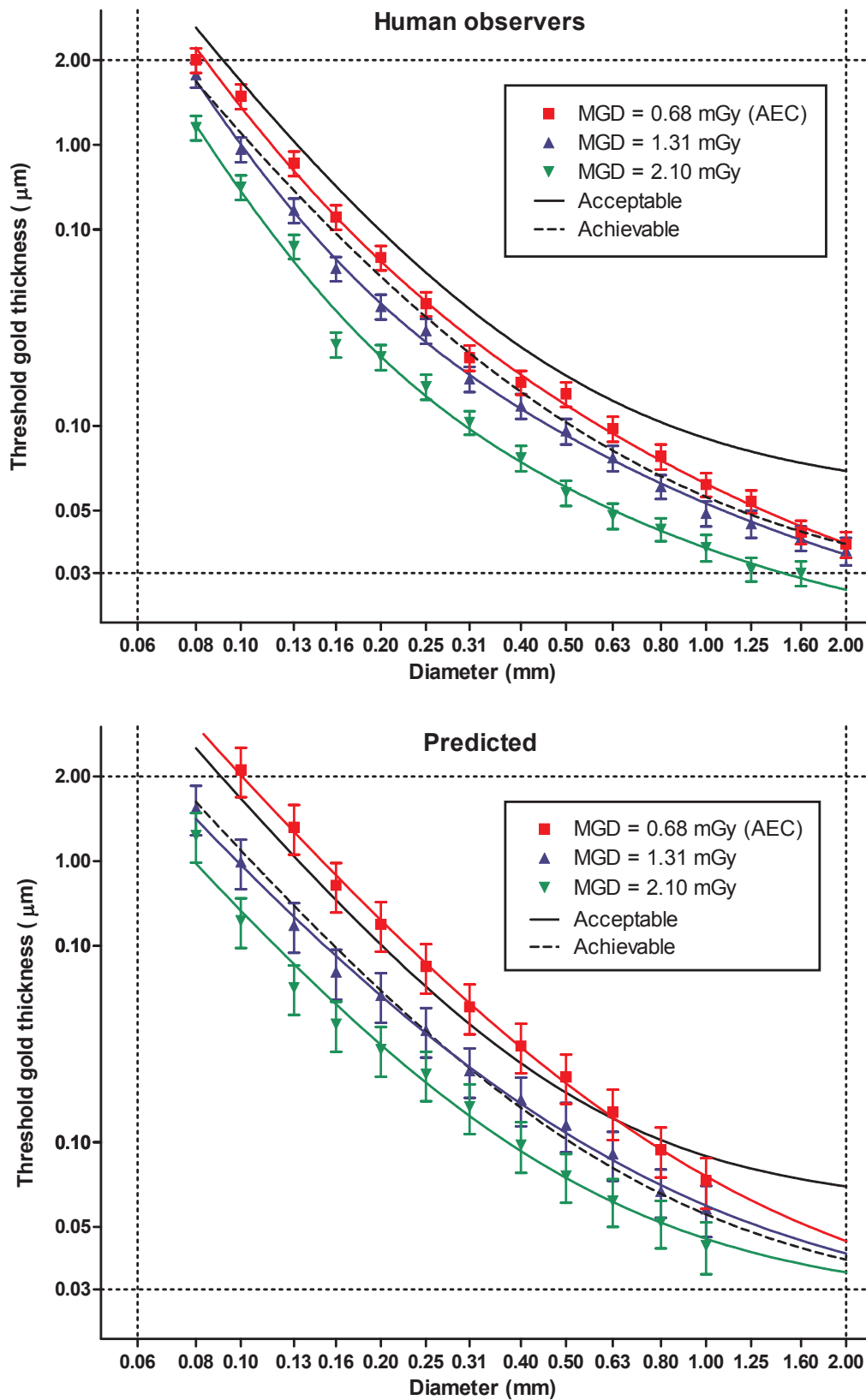


Figure 9 Contrast–detail curves for the system at Cambridge for three different doses at 32 kV W/Rh using human readers and predicted results using automated reading. The 0.68 mGy dose corresponds to the AEC selection. Error bars indicate 95% confidence limits.

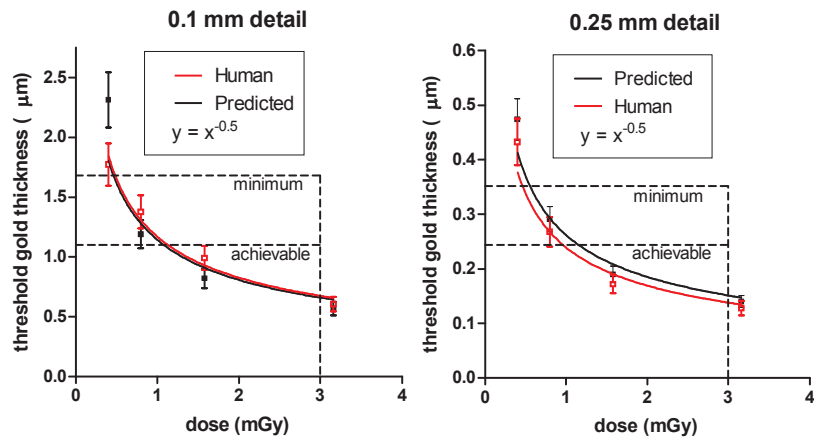


Figure 10a Threshold gold thickness at different doses (Erlangen).

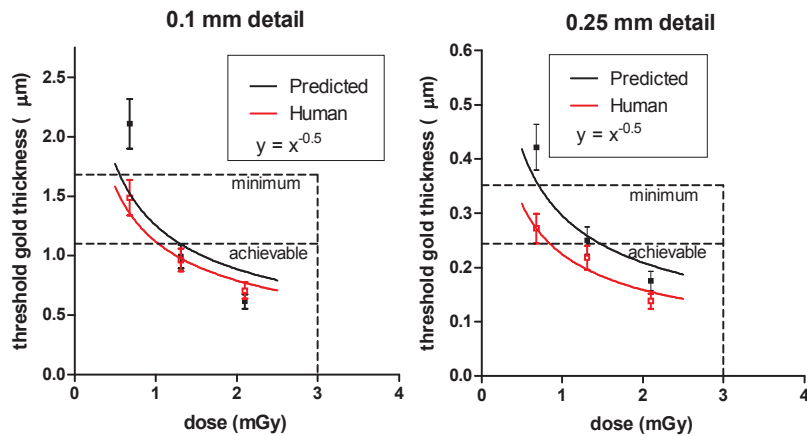


Figure 10b Threshold gold thickness at different doses (Cambridge).

3.5 Comparison with other systems

The MGDs to reach the minimum and achievable image quality standards in the NHSBSP protocol have been estimated from the curves shown in Figure 10. (The error in estimating these doses depends on the accuracy of the curve fitting procedure and pooled data for several systems have been used here to estimate the 95% confidence limits of about 20%.) These doses are shown against similar data for other models of digital mammography system in Tables 6 and 7 and Figures 11–14. The data for the other systems have been determined in the same way as described in this report and the results published previously.^{8–11} The data for film–screens represent an average value determined using a variety of modern film–screen systems.

Technical Evaluation of the Siemens Novation Full Field Digital Mammography System

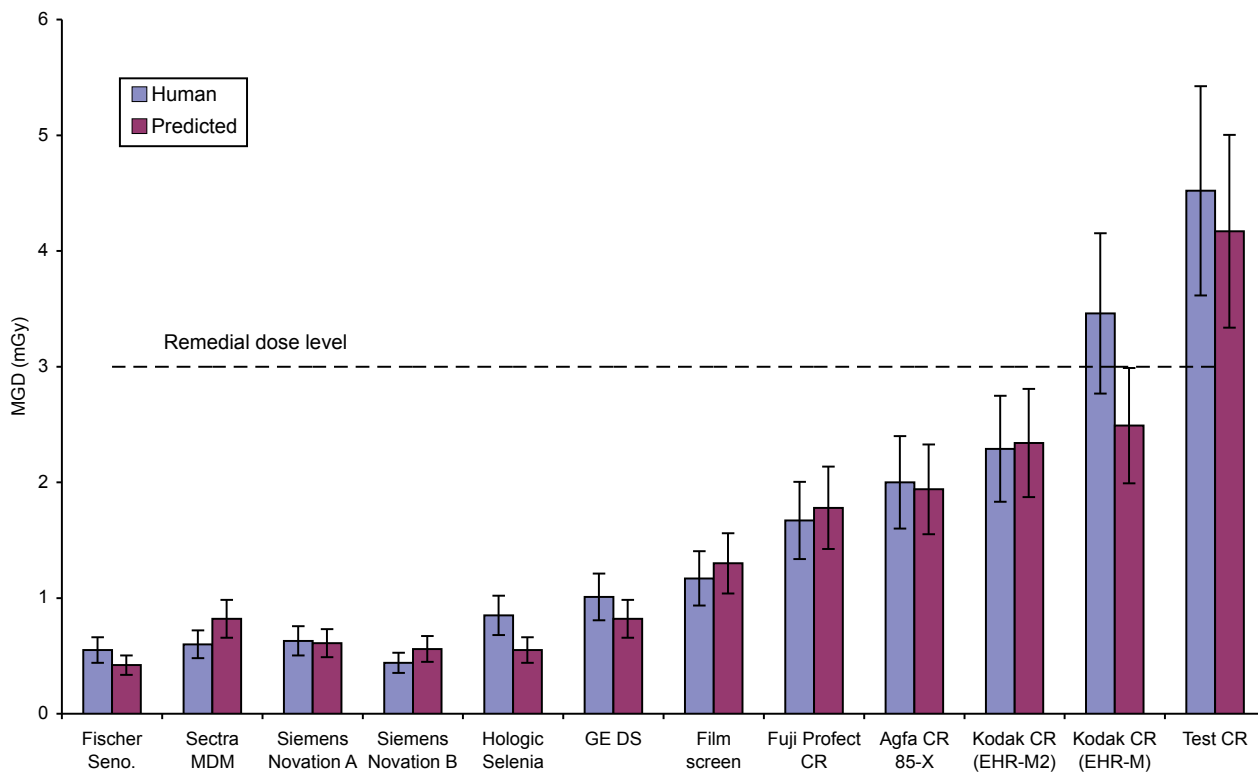


Figure 11 Dose to achieve minimum acceptable image quality standard for 0.1 mm detail. Error bars indicate 95% confidence limits.

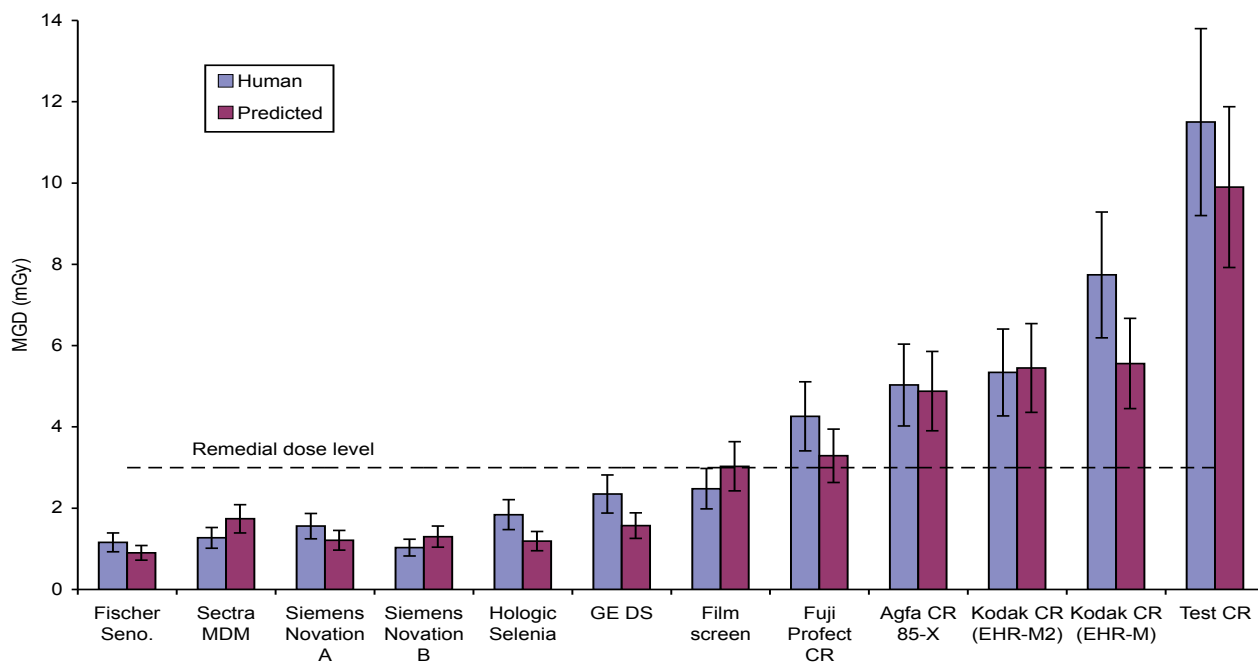


Figure 12 Dose to reach achievable image quality standard for 0.1 mm detail. Error bars indicate 95% confidence limits.

Technical Evaluation of the Siemens Novation Full Field Digital Mammography System

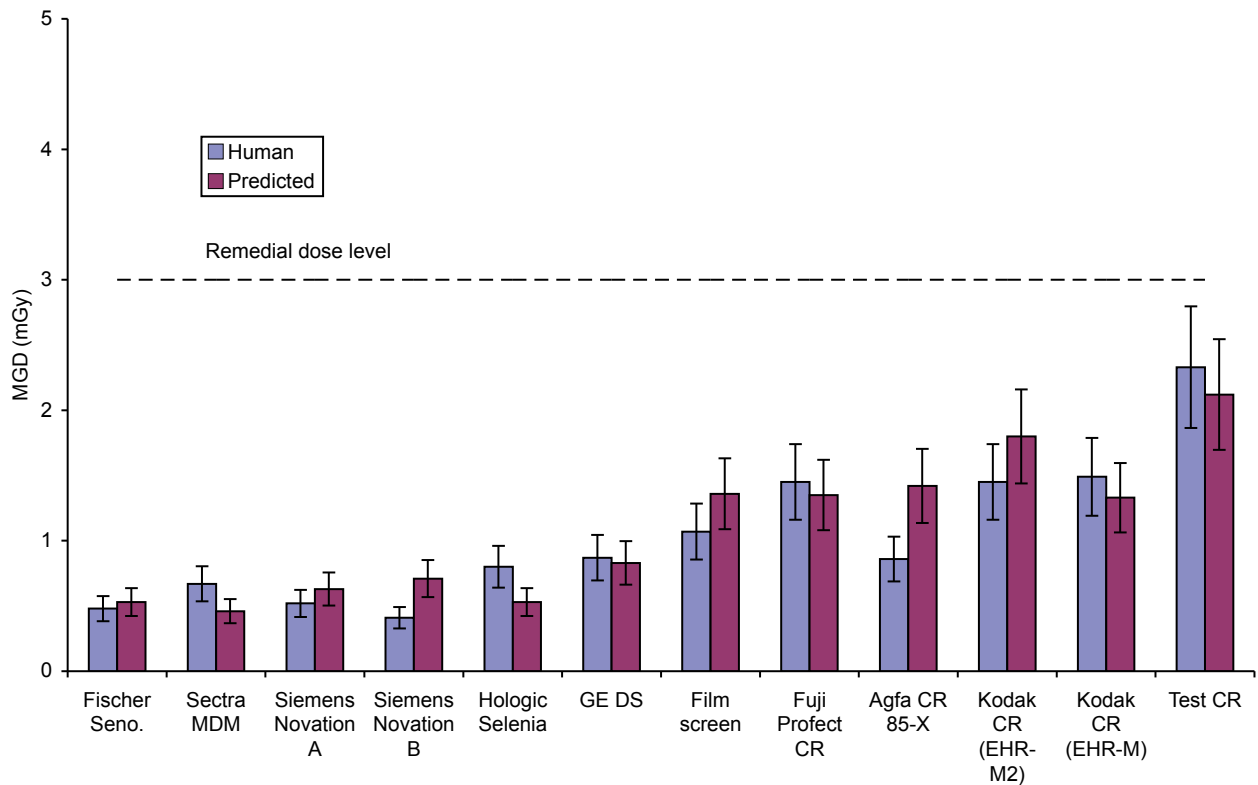


Figure 13 Dose to achieve minimum acceptable image quality standard for 0.25 mm detail. Error bars indicate 95% confidence limits.

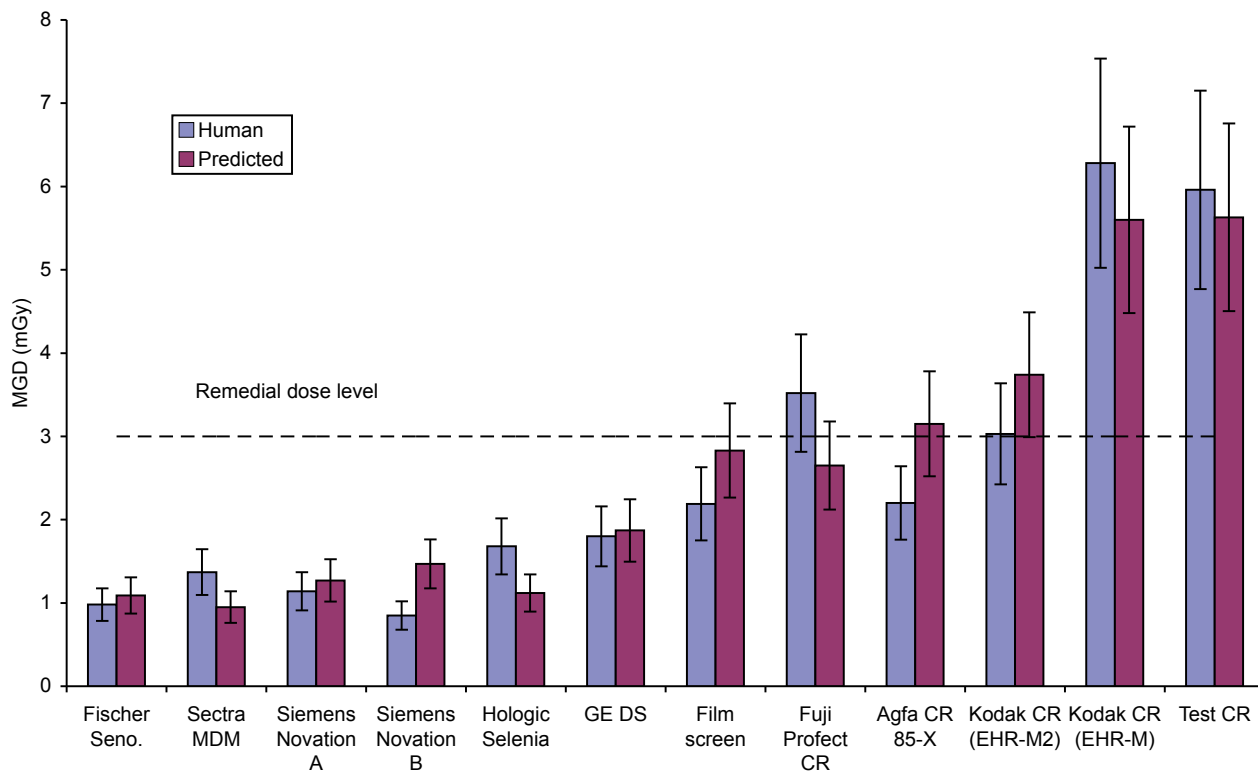


Figure 14 Dose to reach achievable image quality standard for 0.25 mm detail. Error bars indicate 95% confidence limits.

Technical Evaluation of the Siemens Novation Full Field Digital Mammography System

3.6 Optimisation

The optimisation measurements were made on the system at Erlangen but similar results are expected for other Novation systems. The target CNR corresponding to the achievable image quality standard was calculated to be 6.68. The MGDs required to reach this target CNR for each beam quality and thicknesses of PMMA are shown in Figure 15. From these data the optimal beam qualities and mAs were selected and are shown in Table 8.

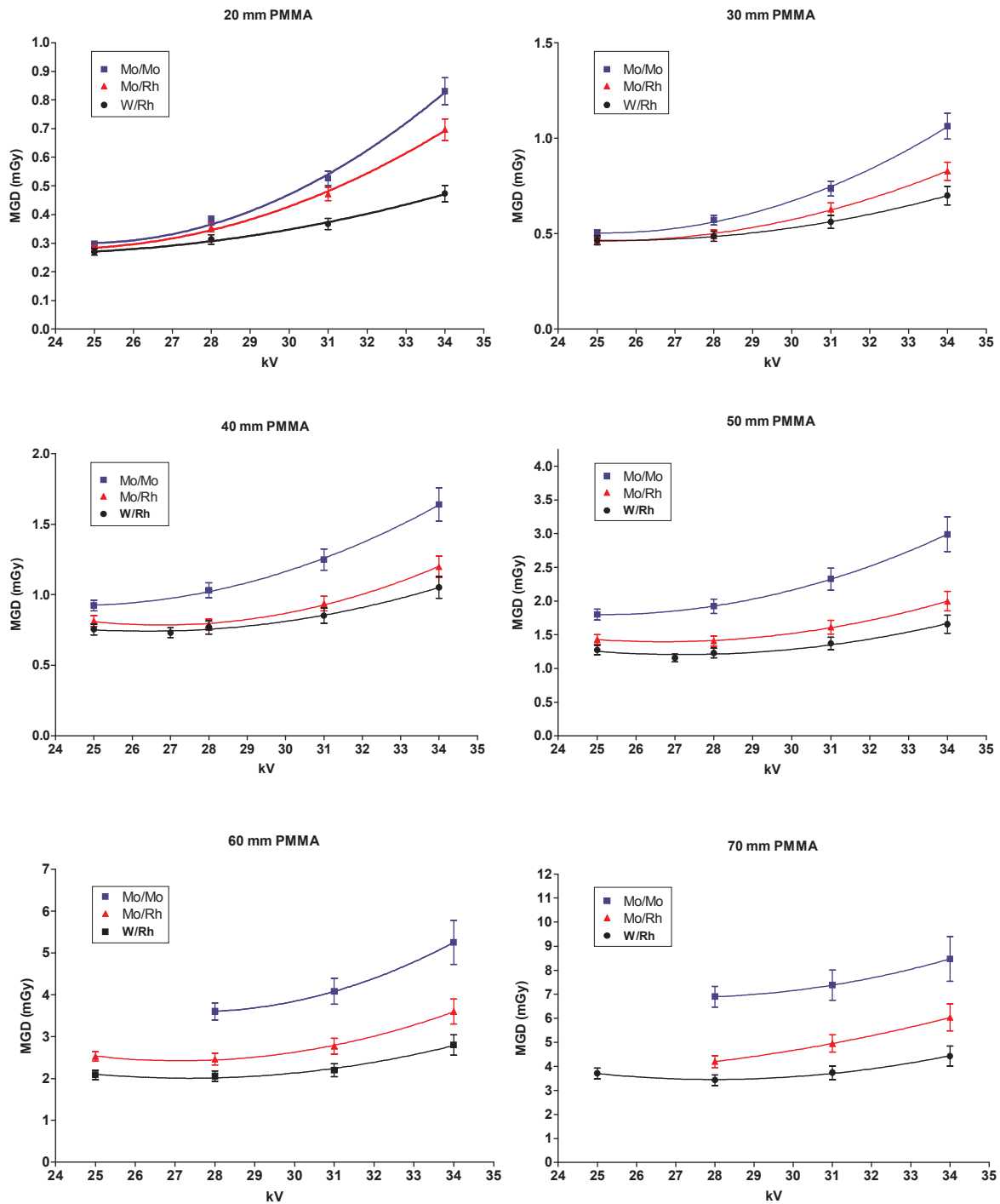


Figure 15 MGD to reach the achievable image quality standard in the NHSBSP protocol (ie $CNR = 6.68$). Error bars indicate 95% confidence limits.

Table 8 Optimal factors to produce achievable image quality (where CNR = 6.68) at the lowest dose

| PMMA thickness | kV target–filter | BGD pixel value | mAs | MGD (mGy) | Dose compared with current AEC selection | Remedial dose level in NHSBSP protocol (mGy) |
|----------------|------------------|-----------------|-----|-----------|--|--|
| 20 | 25 W Rh | 353 | 29 | 0.27 | 95% | 1.0 |
| 30 | 27 W Rh | 428 | 45 | 0.44 | 116% | 1.5 |
| 40 | 28 W Rh | 518 | 84 | 0.77 | 150% | 2.0 |
| 45 | 28 W Rh | 547 | 119 | 1.02 | 156% | 2.5 |
| 50 | 28 W Rh | 547 | 155 | 1.23 | 152% | 3.0 |
| 60 | 28 W Rh | 608 | 295 | 2.06 | 168% | 4.5 |
| 70 | 28 W Rh | 649 | 558 | 3.43 | 201% | 6.5 |

4. DISCUSSION

The detector response was, as expected, linear with a pixel value offset. The noise analysis confirmed that quantum noise is the dominant noise source. The AEC resulted in doses to simulated breasts that were well below the limits in the NHSBSP protocol. The dose for the standard breast simulated with 45 mm of PMMA was 0.65 mGy in Erlangen and 0.71 mGy in Cambridge. These doses are about a quarter of the upper limit of 2.5 mGy applied by the NHSBSP. The doses displayed by both systems were higher than calculated.

The AECs resulted in approximately constant background pixel values of about 360 in Erlangen and 275 in Cambridge. The AECs also chose the W/Rh target filter combination for all thicknesses, with tube voltage selection rising gradually with increasing thickness. The net result of these choices was that the doses were very low and that the contrast and CNR declined with increasing thickness. Comparison with the CNR necessary to reach the achievable and minimum acceptable image quality levels showed that, while excellent image quality can be expected for breasts with small thicknesses, a level close to the minimum acceptable will be achieved for the largest breast thicknesses.

The image quality measurements indicated that for the standard thickness tested (equivalent to 50 mm thickness of PMMA, ie 60 mm of typical breast) the image quality was between the minimum and achievable levels at the current AEC setting. The AEC selected a dose of 0.8 mGy using 28 kV W/Rh at Erlangen and a dose of 0.68 mGy using 32 kV W/Rh in Cambridge. For either system a dose of about 1.25 ± 0.25 mGy was calculated to be necessary to reach the achievable image quality level for this equivalent breast thickness.

The doses required to reach the acceptable and achievable image quality levels were relatively low and broadly similar to other digital radiography systems. The results using the automated image quality assessment were broadly similar to those with human readers and indicate a reasonable degree of consistency between the image quality measurements in this report and others in this series.

The optimisation study found that the W/Rh target–filter combination was preferable for all breast thicknesses. A tube voltage in the range 25–28 kV was always preferable to the use of higher values. This finding is similar to that reported for the Hologic Selenia, which uses a similar detector. The use of a tungsten target with this type of detector seems to yield a dose advantage over a system with only a molybdenum target. These findings suggest that the current AEC design is optimal in terms of beam quality selection but not in terms of mAs. It is suggested that achievable image quality could be reached by increasing the dose by about 50% (see Table 7). This would ensure good image quality for all thicknesses of breast using a dose level that remains well within acceptable limits. It should be noted that at this higher dose level a slightly higher tube voltage may be desirable (eg 31 kV) for the largest breasts to keep exposure times within acceptable limits.

5. CONCLUSIONS

This system is capable of producing excellent image quality for a relatively low radiation dose. As currently set up, the AEC will be satisfactory for most types of breast. The system met the main standards in the NHSBSP and European protocols. However, it is suggested that slightly higher doses would be appropriate, especially for breasts of average and above average thickness.

REFERENCES

1. Workman A, Castellano I, Kulama E, Lawinski CP, Marshall N, Young KC. *Commissioning and routine testing of full field digital mammography systems*. NHS Cancer Screening Programmes, 2006 (NHSBSP Equipment Report 0604).
2. Young KC, Johnson B, Bosmans H, Van Engen R. Development of minimum standards for image quality and dose in digital mammography. In *Digital Mammography, 2005 (IWDM 2004, Proceedings of the Workshop in Durham NC, USA, June 2004)*.
3. Van Engen R, Young KC, Bosmans H, Thijssen M. The European protocol for the quality control of the physical and technical aspects of mammography screening. In: *European Guidelines for Breast Cancer Screening*, 4th edn. Luxembourg: European Commission, 2006.
4. Young KC, Cook JH, Oduko JM. Use of the European protocol to optimise a digital mammography system. In: Astley SM, Bradey M, Rose C, Zwiggelaar R (eds). *Proceedings of the 8th International Workshop on Digital Mammography. Lecture Notes in Computer Science*, 2006, 4046: 362–369.
5. Young KC, Oduko JM, Bosmans H, Nijs K, Martinez L. Optimal beam quality selection in digital mammography. *British Journal of Radiology*, 2006, 79: 981–990.
6. Young KC, Cook JH, Oduko JM, Bosmans H. Comparison of software and human observers in reading images of the CDMAM test object to assess digital mammography systems. *Proceedings of SPIE Medical Imaging*, 2006, 614206: 1–13.
7. Young KC, Cook JH, Oduko JM. Automated and human determination of threshold contrast for digital mammography systems. In: Astley SM, Bradey M, Rose C, Zwiggelaar R, editors. *Proceedings of the 8th International Workshop on Digital Mammography. Lecture Notes in Computer Science*, 2006, 4046: 266–272.
8. Young KC, Oduko JM. *Evaluation of Kodak DirectView Mammography Computerised Radiography*. NHS Cancer Screening Programmes, 2005 (NHSBSP Equipment Report 0504).
9. Young KC, Oduko JM, Woolley L. *Technical Evaluation of the Hologic Selenia Full Field Digital Mammography System*. NHS Cancer Screening Programmes, 2007 (NHSBSP Equipment Report 0701).
10. Young KC, Oduko JM. *Technical Evaluation of Kodak DirectView Mammography Computerised Radiography System using EHR-M2 Plates*. NHS Cancer Screening Programmes, 2007 (NHSBSP Equipment Report 0706).
11. Young KC, Oduko JM. *Technical Evaluation of Agfa CR-85 Mammography System*. NHS Cancer Screening Programmes, 2007 (NHSBSP Equipment Report 0707).